Jurnal Tribologi 28 (2021) 32-47

A rough surfaces deformation in grease lubricated roller bearing

Nurul Farhana Mohd Yusof *, Foo Chun Yit

School of Mechanical Engineering, Universiti Sains Malaysia, 14300 Nibong Tebal, Pulau Pinang, MALAYSIA.
*Corresponding author: mefarhana@usm.my

KEYWORDS

Rough surface
Asperities
Grease
Surface roughness
Surface deformation
Rolling contact

ABSTRACT

The contact between two surfaces predominantly is contact between rough surfaces consisting of many asperities or surface irregularities. Surface deformation in the early cycles of the rolling contact occurs at a micro asperities level and hard to be assessed due to the minimal changes. Several works describe the surface asperities deformation in dry condition; however, the deformation with the presence of lubricant has not been reported. This study aims to characterize the deformation of the rough surfaces in dry and lubricated condition. Experimental work is carried out using a rolling element bearing test rig. The surface deformation is measured using an online technique and surface characterization is carried out on the bearing's inner race surface. The rough surface deformation is attributed to reducing asperities peaks height due to plastic deformation and wear. The un-lubricated bearing condition accelerated the surface damage with surface roughening, indentation and material accumulation. Roughness measurement shows that the skewness and kurtosis parameters provide a better representation of rough surfaces and can differentiate between surfaces having different shapes but similar R_a value. With grease lubrication, 0.79 μm of film thickness is formed between two contacting surfaces and prolong the bearing life.

Received 7 October 2020; received in revised form 4 January 2021; accepted 20 February 2021.
To cite this article: Mohd Yusof and Yit. (2021). A rough surface deformation in grease lubricated roller bearing. Jurnal Tribologi 28, pp.32-47.

1.0 INTRODUCTION

The contact between two surfaces predominantly is contact between rough surfaces consisting of many asperities or surface irregularities. The study of surface contact was pioneered by Hertz in 1882 by considering two elastic bodies where the area of contact is determined based on the contacting surface geometry such as point, elliptical and line contact (Johnson, 1985). Archard (1957) presented a more realistic model of rough surfaces, described as a hierarchical model consisting of small spherical bumps on top of larger spherical bumps and the area of real contact is proportional to the load. However, the model cannot be used practically because this model cannot accurately represent real surfaces. Greenwood and Williamson, (1966) presented an improved model based on the contact between rough and smooth surfaces. The model is based on Hertzian elastic contact where the surface asperity distribution was assumed Gaussian with a constant radius of asperity summits. Greenwood and Tripp, (1967) expanded the model to the contact between two rough surfaces and concluded that there is no significant difference between the contact of a rough surface and a flat plane. Bush et al., (1975) refined the theory by assuming that roughness exists at different length scales with variation in radius, height and ellipticity. The real measured asperities have been applied in the finite element model to observe the influence of adjacent asperities in contact (Bryant et al., 2012). Recent work started to investigate the change in contact area regarding the film thickness ratio, considering the surface roughness parameter (Tomota et al., 2019; 2020).

The experimental work on the deformation of rough surfaces asperities during contact have been carried out extensively. Berthe et al., (2014) monitored the asperities deformation in the rollers subjected to line contact. They observed that the contact area of the rough and smooth disc increases with the reduction of the asperities height. The experiment using twin disks made of hardened alloy steel subjected to rolling/sliding contact shows that the asperity peaks were blunted with a small change of the valleys after rolling contact (Clarke et al., 2016). Measurement on gear surface found that both peak and valley of surface asperities were deformed but most of the changes occur at the highest peaks (Sosa et al., 2014; 2016). In point contact, the surface asperities are stiffer if their surface lay direction is parallel to the rolling direction (Tasan et al., 2007). Recently, the effect of loading on the deformation of surface asperities, the evolution of the real contact area and roughness parameters were analyzed experimentally and numerically (Kucharsky and Starzynki, 2019). The real contact area and asperity deformations for different materials and roughnesses are also investigated (Brodnik and Kalin, 2020). However, detailed information on the surface condition related to asperities deformation and roughness is unknown.

Lubrication plays an important role to form a layer to separate the contact between rough surfaces. Insufficient lubrication may cause direct contact between asperities peak, thus accelerating surface degradation and increasing friction between two contact surfaces (Mohd and Ripin, 2014). A mapping of rough surface contact in elastohydrodynamic lubrication in a ball-on-disc machine has been presented where the resulting friction and average surface roughness of the ball are presented (Hansen et al., 2019). Surface deformation in the early cycles of the rolling contact occurs at micro asperities level and hard to be assessed due to the minimal changes. Several works describe surface deformation in dry condition (Jamari and Schipper, 2007a; 2007b; Tasan et al., 2007; Berthe at al., 2014; Sosa et al., 2014, 2016; Clarke at al., 2016); however, the micro asperities deformation in lubricated condition has not been reported.

The purpose of this paper is to characterize the rough surface deformation in dry and lubricated condition. The measurement is carried out using online method by scanning the sample

directly under the microscope at a fixed reference datum to ensure that the similar surface is scanned in each rolling cycle. The importance of this work is asperity peaks and valleys deformation are related to the roughness parameter including average roughness, skewness and kurtosis. The finding aims to produce an idea of the rough surface condition indicated by the various roughness parameters. This may reduce time in the rough surfaces measurement as it requires high precision equipment and experimental setup due to micro-scale deformation. This work also presents how lubricant work on micro asperities to reduce surface damage. The knowledge is crucial to understand how the lubricant encounters the rough surface asperities with various peaks height and provide a prognosis of surface damage with the presence of lubricant.

2.0 MATERIALS AND METHODS

2.1 Experimental Setup

The experiment was carried out using a rolling element bearing test rig. The test rig is designed and fabricated in-house. The experimental rig consists of cylindrical roller bearings, support bearings, shaft, coupling, AC motor, motor controller and load holder as shown in Figure 1 (a). The shaft was supported by pillow blocks and driven by an AC motor. The speed of the AC motor was controlled by a speed controller. The shaft was set at 1500 rpm and a load of 98 N was given. The load on the bearing was applied by attaching the 10 kg dead weight at the load holder. A screw is mounted at the centre of the bearing housing, supporting the load to produce a load concentration in the middle of the bearing width as shown in Figure 1 (b) and Figure 1 (c). The purpose is to find the effect of the load position on the line contact surface deformation. The bearing components consist of the inner race, outer race, rollers and cage. During operation, line contact occurs between the roller and inner race surface (Johnson, 1987; Wang and Chung, 2013). Load setup configuration in this experiment is expected to produce higher contact stress at the centre of the bearing surface. The experiments are carried four times for each dry and grease conditions. The specification of the cylindrical bearing is shown in Table 1.

Table 1: Specification of cylindrical roller bearing.

Components	**Dimension**
Number of rollers	13
Roller diameter (d_r)	7.5mm
Roller length (L_r)	10mm
Inner race diameter (D_i)	25mm
Outer race diameter (D_o)	52mm
Pitch diameter (d_m)	38.5mm
Width of bearing (B)	15mm
Roller and inner race material	52100 Stainless steel
Poison's ratio (v)	0.3
Young modulus of elasticity (E)	210GPa

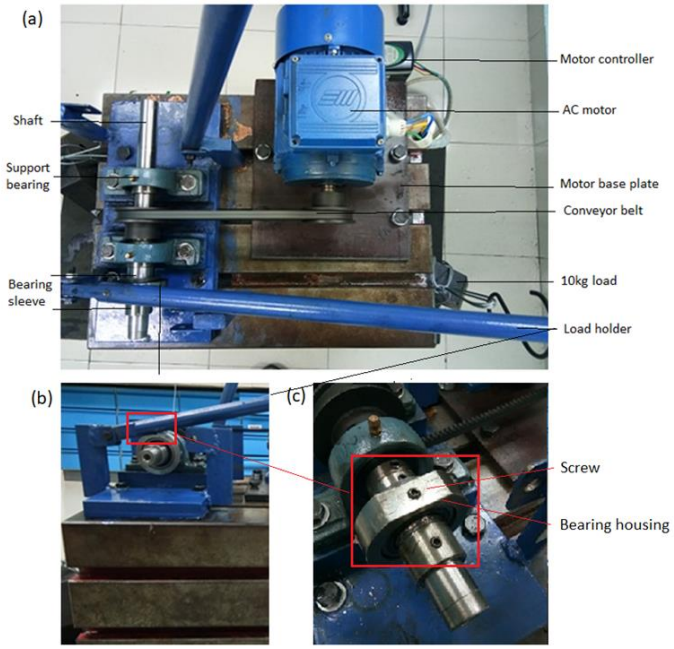

Figure 1: Experimental setup.

2.2 Surface Characterization

Surface characterization is performed using an Infinite Focus Microscope (IFM). The inner race was removed every 30 minutes and 10 hours for dry bearing and lubricated bearing respectively. The dry un-lubricated bearing characterization performed more frequently as the early failure of the bearing is expected. The inner race is cleaned using acetone, and then the surface was scanned at 10x magnification as shown in Figure 2. The reference mark is identified every time the surface is scanned to ensure the same location is measured at different rolling cycles. Therefore, the surface topography, profiles and roughness parameters are measured throughout the scanning line of 10 µm length.

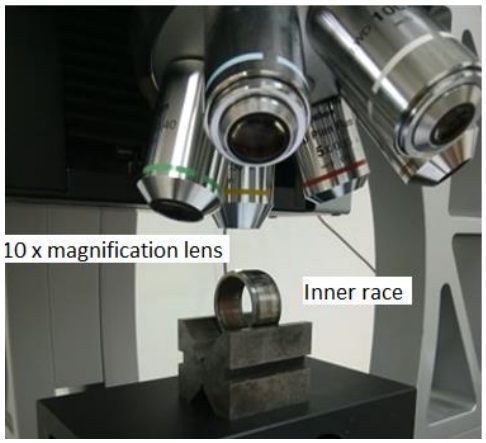

Figure 2: Scanning of inner race surface.

2.3 Surface Parameter

Roughness parameters are widely used to describe asperities height distribution quantitatively. The surface roughness profile consisting of asperities peak and valley height distribution is measured and the average roughness (R_a), surface kurtosis (R_{ku}) and surface skewness (R_{sk}) parameters are monitored. Average roughness is the average absolute deviation of the roughness irregularities or known as asperities over the mean line in one sample length (Gadelmawla et al., 2002). Skewness and kurtosis parameters are important as it shows a better representation of a rough surface (Thomas, 1981), and can be used to differentiate between surfaces having different shapes but similar R_a value (Gadelmawla, 2002). Therefore, these parameters can describe the asperities height distribution and potential tribological contact behaviour. Existing work on the simulation of various asperity shapes show that the wear volume changes are larger with smaller asperity width, indicating the asperity with a sharper peak will deform easier (Yastrebov et al., 2011). The skewness of surface height distribution is used to measure the symmetry of the surface roughness profile about the mean line. Generally, the surface heights are normally distributed. With positive skewness, the roughness profile consists of many high peaks and valleys are filled in, or the peaks are away from the mean line. Kurtosis of the roughness profile is used to measure the sharpness of the roughness distribution and describe the shape of the profile. The surface heights are normally distributed throughout the surface if the kurtosis is equal to 3.

The mathematical formulas used to calculate the average roughness (R_a), skewness (R_{sk}) and kurtosis (R_{ku}) of the profile are as follows (Gadelmawla, 2002):

$$R_a = \frac{1}{n}\sum_{i=1}^{n} y_i \tag{1}$$

$$R_{sk} = \frac{1}{NR_q{}^3}\sum_{i=1}^{N} Y_i{}^3 \tag{2}$$

$$R_{ku} = \frac{1}{NR_q{}^4}\sum_{i=1}^{N} Y_i{}^4 \tag{3}$$

Where n is the number of s along the measurement length, N is the number of point, R_q is the root mean square roughness parameter and Y_i is the height of profile at point number i.

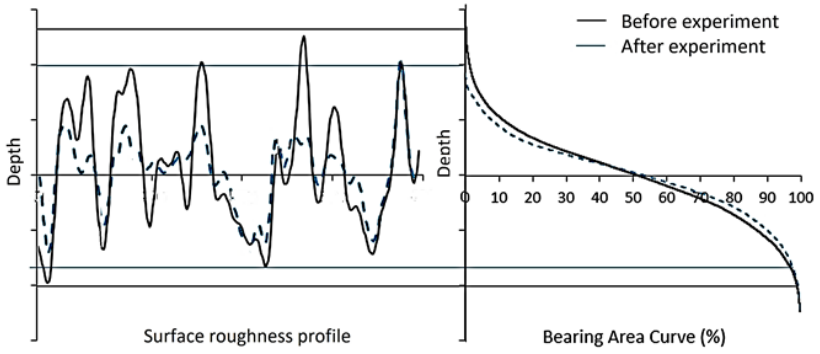

Figure 3: Surface roughness profile and the related BAC.

Another method used to describe rough surfaces is Bearing Area Curve (BAC). BAC is the integration of asperities width over asperities depth for a given sample length, which is presented as an asperity height cumulative percentage (Abbot and Firestone, 1933) as shown in Figure 3. BAC is used to estimate the proportion of the nominal area between the surfaces of inner race and rollers that are in real contact (Sahoo, 2011). A steep gradient indicates asperities with various heights, whereas a gentle gradient indicates more uniform surface asperities (Rasp and Wichern, 2002).

2.4 Lubricant Film Thickness

In this study, the bearings were run in unlubricated and lubricated conditions. For dry unlubricated condition, the whole bearing was cleaned and submerged into acetone to remove oil. Grease was applied to lubricate the bearing and relubrication was carried out periodically when the bearing was remount after surface scanning. The grease used is SKF LGMT 2/0.4 and the specification is shown in Table 2.

Table 2: Specification of grease.

Item	Properties
Brand of grease	LGMT 2/0.4
Base oil type	Mineral
Soap type	Lithium
Base of viscosity	
40°C	110mm^2/s
100°C	11mm^2/s
Operating temperature range	–30 to +120 °C
Absolute viscosity (η_o)	0.09Ns/m^2
DIN 51825 code	K2K-30
Colour	Red Brown

The lubricant film thickness for the roller bearing was calculated using Dowson and Higginson's (1959) equation and later modified by Pan and Hamrock (1989), as shown in equation (4), (Bruce, 2010)

$$h_{min} = 1.714U^{0.0694}G^{0.568}W^{-0.128}R \quad (4)$$

Where;

Speed parameter
$$U = \frac{\eta_0 \mu_0}{E'R} \quad (5)$$

Material parameter
$$G = \varepsilon E' \quad (6)$$

Load parameter
$$W = \frac{F}{E'R} \quad (7)$$

Where η_o is absolute viscosity, u_o is surface velocity, E' is effective modulus of elasticity, R is radius of curvature, ε is material coefficient, F is Load per length.

The surface velocity, u_o can be calculated using equation (8) as follows.

$$U_0 = \frac{u_1 + u_2}{2} \tag{8}$$

$$U_1 = \frac{2\pi R_1 N}{60} \tag{9}$$

$$U_2 = \frac{2\pi R_2 N}{60} \tag{10}$$

Where U_1 is the surface velocity of bearing, U_2 is the surface velocity of roller, R_1 is the radius of inner race bearing, R_2 is the radius of roller, and N is the motor speed.

Effective modulus of elasticity, E' can be calculated using equation (11) as follows:

$$\frac{1}{E'} = \frac{1}{2}\left[\frac{1 - V_1^2}{E_1} + \frac{1 - V_2^2}{E_2}\right] \tag{11}$$

Where V_1 is the Poisson's ratio of the inner race material, V_2 is the Poisson's ratio of the roller material, E_1 is the young modulus of inner race material and E_2 is the young modulus of roller material.

Radius of curvature, R can be calculated using equation (12) as follows:

$$\frac{1}{R} = \frac{1}{R_1} + \frac{1}{R_2} \tag{12}$$

Where R_1 is the radius of inner race bearing and R_2 is the radius of roller.

From the calculation, the film thickness of the grease in roller bearing is obtained at 0.79 μm.

3.0 RESULTS AND DISCUSSION

3.1 Surface Characterization and Surface Profile Analysis

Figure 4(a) and Figure(b) show the images of inner race surfaces running in un-lubricated conditions before and after the experiment. The surface roughness profiles are shown in Figure 4(c). Overall, the surface roughness profile shows that after the experiment, the asperities height becomes non-uniform with deep valleys and high peaks. The applied load is shown at the position of 5 mm of the measurement length. The figure shows uniform surface roughness characteristics initially, as shown in Figure 4(a). After the bearing running in dry un-lubricated condition for 90 minutes, the roller bearing shows a sign of failure with a production of high noise, vibration and spark. Surface scanning shows that the bearing's inner race is damage, and some discolouration appears with brown, white and black colour. The brown colour is typically due to overheating, which can be related to Welzel, (2009) where the spark is produced when the contact surface temperature is very high. The surface profile shows that the indentation occurs at the brown colour area with a formation of a wide valley with 2 μm depth. A deeper valley with 4.5 μm depth is observed at the white colour area, which is at the applied load position. The effect of high load can be seen here, and this can be related to Singh et al., (2019) where the wear depth increases with an increase in normal load. It was observed that the depth of wear track became deeper with an increase of sliding cycles (Lee et al., 2019). At the black colour area, the surface profile shows

a high peak. It is anticipated that with the absence of lubricant, the removed particles from the load concentration area at the centre have been pushed away to the side and then accumulating to become a large peak.

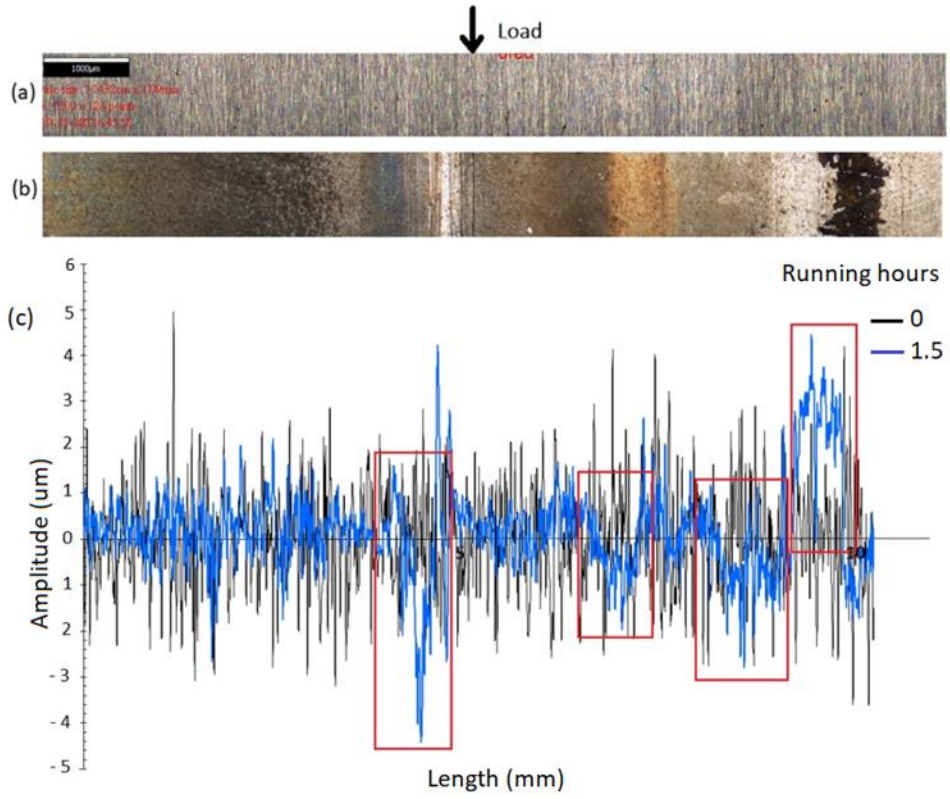

Figure 4: Surface scanning of the dry un-lubricated inner race (a) before and (b) after the experiment and (c) the surface roughness profiles.

The image of inner race surfaces running in grease lubricated condition before and after the experiment is shown in Figure 5(a) and(b) respectively. The experiment was stopped after 100 hours as minor vibration was observed on the bearing. A comparison of both surface images shows that surface deformation occurs less severe than an un-lubricated bearing surface. There are many scratch lines and discolouration appear in brown. It is expected due to the grease's heating due to excessive load and continuous contact. The surface roughness profiles become non-uniform throughout the scanning length as seen in Figure 5(c) and most of the asperities peak height is reduced after 100 hours. The valley depth increases at the applied load and few adjacent areas. The asperities deformation in the early cycles of rolling contact is attributed to the material removed from the asperity peaks due to plastic deformation and wear (Ismail *et al.,* 2011; Mohd and Ripin, 2016). In dry contact condition, 66 % of asperities height deformation is due to plastic deformation and 34 % wear. This occurs with the nominal maximum Hertzian contact pressure of 209 MPa (Mohd and Ripin, 2016) and the percentage may vary with different contact pressure. The material particles removed from the load concentration area are observed minorly attached

to the surface as the lubricant can wash away the removed material (Groover, 2010). Grease forms a film thickness to separate the contact between surfaces and plays an important role in eliminating the particles generated from the asperities contact. Therefore, there is no material accumulation of removed material particles found on the lubricated bearing's surface.

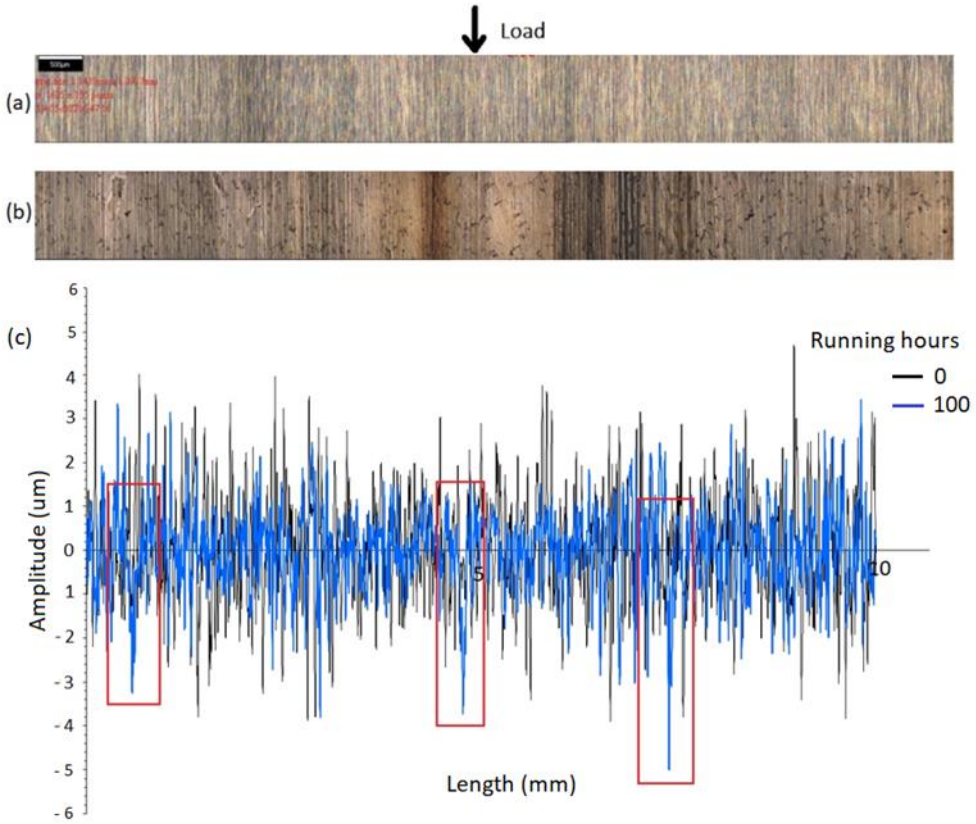

Figure 5: Surface scanning of the grease-lubricated inner race (a) before and (b) after the experiment and (c) the surface roughness profiles.

Surface topography characterization is carried out for a further understanding of the surface deformation. Figure 6 (a) and (b) show damage un-lubricated surface and Figure 5 (c) and (d) show damage grease-lubricated surface. The figures verified that the surface indent occurs at the applied load area with 5 µm and 3 µm depth for un-lubricated and lubricated bearings respectively. There is a groove formed as an effect of high load. The accumulation of materials with the absence of lubricant is seen in Figure 6 (b). High temperature has a significant effect on increasing the rate of plastic deformation because the material's yield strength is lower at a higher temperature; therefore, the peaks were removed and added at a fast rate. This causes the changes of surface roughness (Wei et al., 2009). It is expected that the material particles from wear and plastic deformation of high asperities peak contribute to the material accumulation. With lubrication, surface indent also occurs at the load concentration area after a long operation period; however, the surface deformation rate is slower. Figure 6(d) shows the surface roughening that take place adjacent to the load concentration area. As the surface asperities were

removed, it may fall to the adjacent location then rolled away during the rolling contact, thus resulting in a change of surface roughness.

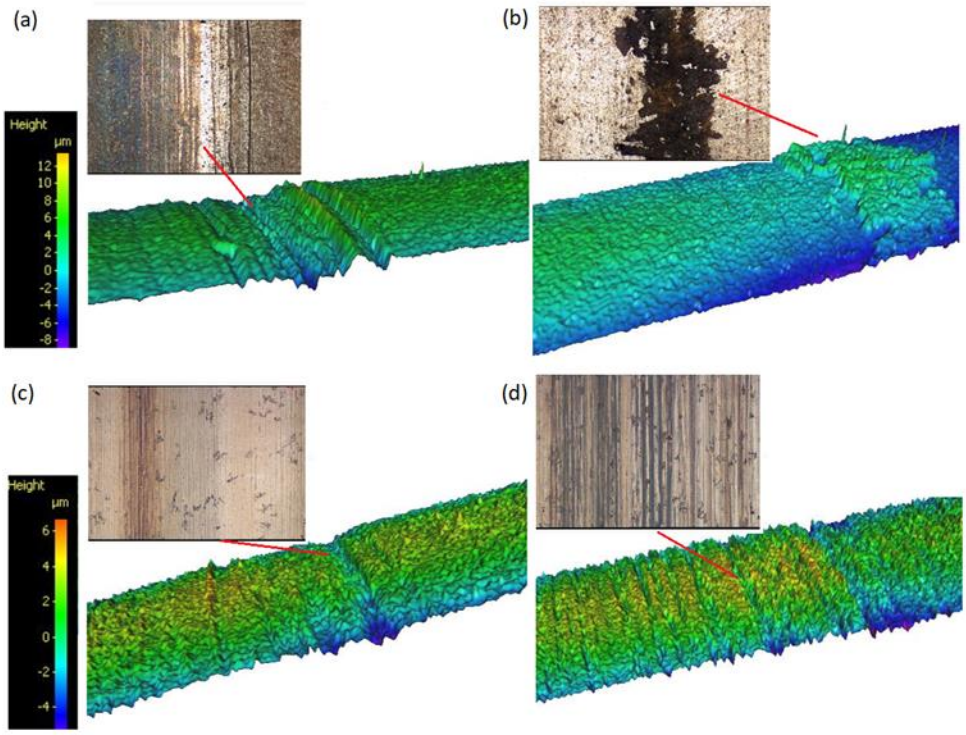

Figure 6: Surface topography of the damage (a) and (b) un-lubricated (c) and (d) lubricated bearings.

3.2 Surface Roughness Analysis

The average surface roughness of the inner race before and after the experiment is shown in Figure 7. For dry un-lubricated condition, the R_a value is decreased initially from 0.51 µm to 0.45 µm, then rising back to 0.5 µm. Based on the R_a value, the surface asperities change 11.74 % from the original surface condition. The reduction of surface roughness in a rolling contact normally due to the effect of the surface polishing process (Mohd and Ripin, 2014). However, the roughness may rise back due to the rolling of removed particles, the high difference between surface asperities peak and valley height, the formation of denting, micro pitting and the presence of contaminant sticking on the surface. By comparing with the scanned surfaces in Figure 4 and Figure 5, it is expected that the rising of surface roughness is due to the formation of deep valleys and materials accumulation on the surface that contributes to the massive height difference. The R_a of the lubricated surface is reduced consistently from 0.51 µm to 0.485 µm, which is 4.9 % reduction. The reduction of surface roughness is due to surface polishing of the asperities peak height, and the presence of lubricant preventing the removed material particles from accumulating on the surface. There is not much difference between the final roughness values of two operating conditions, even though the surface damage is significantly different. The finding indicates that the R_a parameter is not suitable to represent the surface condition independently.

The surface condition of the un-lubricated surface is severely damaged with groove and material accumulation.

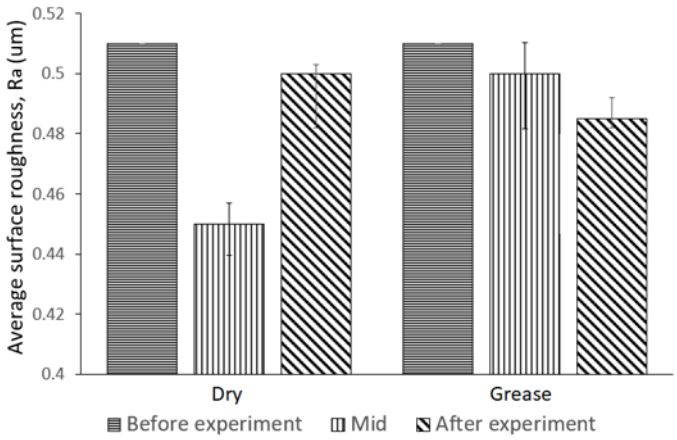

Figure 7: Average surface roughness of dry un-lubricated and grease-lubricated bearings.

Figure 8 shows that the skewness of the inner race surface is positive initially at 0.06, which is close to 0, indicating that the initial surface heights are normally distributed. However, it decreases to a negative value of -0.076 during the surface polishing process. This shows that the peaks are removed, and the valleys are filled in with the removed material during the polishing process, in line with the surface roughness reduction. The negative skewness has been observed by Ray and Roy, (2011) with the existence of many deep valleys and peaks removed from the asperities height with more peaks close to the mean line. At the end of the experiment, the surface skewness for dry bearing increase abruptly to 0.89 in line with the presence of surface damage. A high R_{sk} value indicates that the surface is non-uniform throughout the scanning area. This is because the surface damage is more severe at a certain location such as the indentation groove at the centre and the material accumulation at one side. For the grease-lubricated bearing, the skewness decreases continuously to -0.36 at the end of the experiment. This indicates that the asperities peak was removed, and more valleys were found on the surface. As compared to the scanned surface image in Figure 4, the reduction of R_{sk} value is due to the formation of small valleys and surface indentation. This indicates that the skewness parameter can be used to evaluate surface roughness asperities peak and valley conditions.

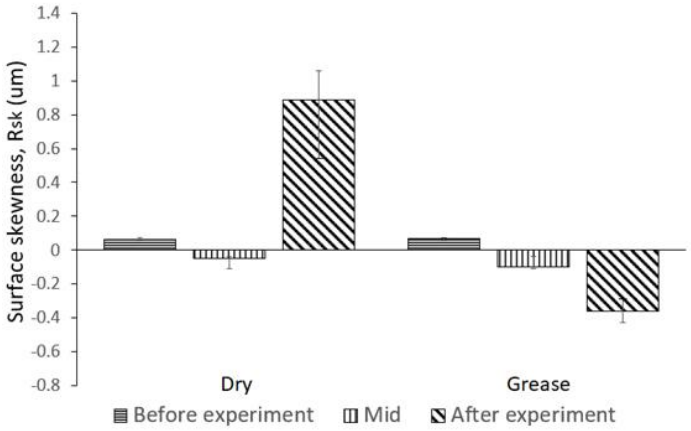

Figure 8: Surface skewness of dry un-lubricated and grease-lubricated bearings.

Figure 9 shows that the R_{ku} value of the inner race surface before the experiment is 3.18 which is close to 3. The surface heights are normally distributed throughout the surface if the kurtosis is equal to 3, thus indicates that the surface heights are almost normally distributed initially. Without lubrication, the R_{ku} value increases tremendously to 5.85 at the end of the experiment. The R_{ku} value more than 3 represents the surface has many high peaks and low valleys. On the other hand, for the profile with kurtosis less than 3, the surface has few high peaks and low valleys (Gadelmawla et al., 2002). This shows that the R_{ku} parameter is in good agreement with R_{sk} parameter with more high peaks and deep valleys on the surface. This also represents that the surface of a dry un-lubricated inner race becomes non-uniform. The kurtosis value of lubricated bearing increase marginally indicates the rate of surface modification or degradation is slower. The polishing and roughening processes at certain locations, as seen in Figure 5, contribute to the rising of the high peaks and low valleys. At the end of the experiment, the kurtosis reaches the maximum value of 4.25 which is much lower than the dry surface. Therefore, it can be concluded that the R_{ku} parameter effectively describes the presence of abnormal peak height and valley depth in the surface asperities profile.

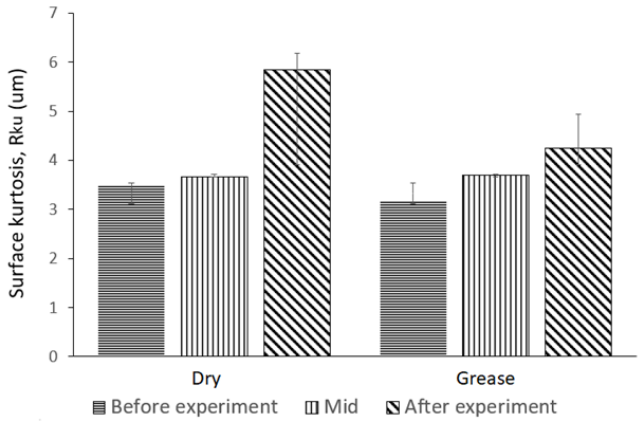

Figure 9: Surface kurtosis of dry un-lubricated and grease-lubricated bearings.

Figure 10 shows the BAC curves before and after the experiment for (a) un-lubricated and (b) lubricated bearings. It is observed that the curve slope becomes less steep after the contact. This is due to lower surface asperities formed after the contact. The relation of curve slope and asperities profile is shown previously in Figure 3. The BAC gradient decreases from 0.033 to 0.023; however, there is an abnormal curve shape at the first 10% of BAC, representing abnormal high asperities peak. This is expected due to material accumulation that has been observed in the surface profile and topography in Figure 4(c) and Figure 6 (b). The BAC curve also becomes less steep for the lubricated bearing where the curve gradient reduces from 0.048 to 0.038. Previous studies explained that the reduced gradient phenomenon could attribute to wearing and/or plastic deformation of surface asperities (Cabanettes and Rosen, 2014; Olofsson and Dizdar, 1998; Rasp and Wichern, 2002; Suh et al., 2003; Sosa et al., 2016). A steep gradient indicates asperities of rapidly varying heights, whereas a gentle gradient indicates asperities with more uniformly distributed height where the height change is more gradual (Rasp and Wichern, 2002). This indicates that the BAC curve can be used to describe the surface height condition. According to Sahoo, (2011), BAC is used to estimate the proportion of the nominal area between the surfaces of inner race and rollers that are in real contact. From the current finding, the nominal contact area between inner race and rollers is expected to increase and more surface area involved in supporting the load.

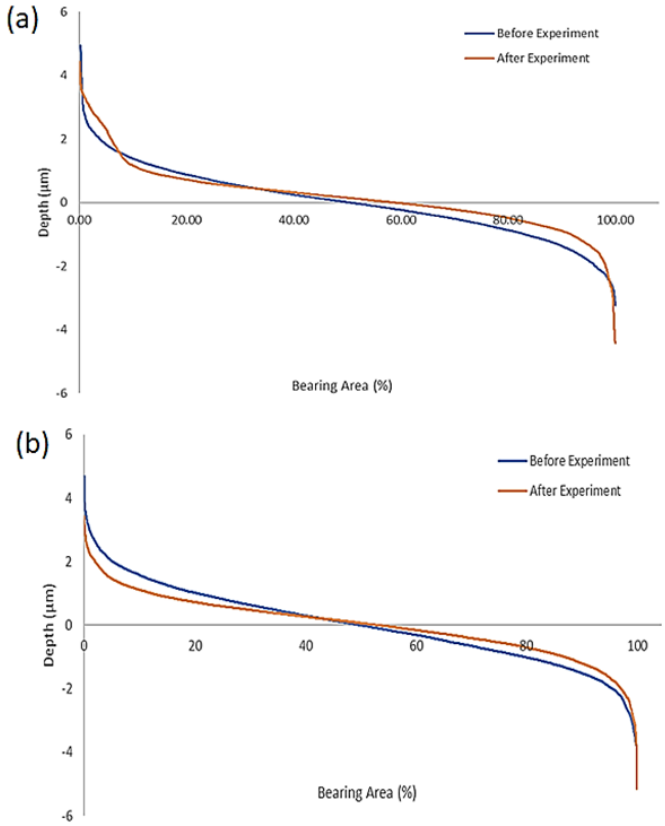

Figure 10: BAC of (a) un-lubricated (b) lubricated bearings.

4.0 CONCLUSIONS

In this work, rough surface deformation in grease lubricated roller bearing has been investigated by surface characterization on the bearing's inner race surface. From the finding, the following conclusions can be drawn:

(a) The rough surface deformation is attributed to reducing asperities peaks height due to plastic deformation and wear. Surface topography shows 5 μm and 3 μm depth difference from peak to the valley for un-lubricated and lubricated bearings, respectively. The R_a measurement shows 11.74 % and 4.9 % reduction for dry un-lubricated and grease-lubricated condition, respectively; however, the R_a value for the dry bearing rises back due to surface damage. The R_{sk} final value of un-lubricated bearing increase 93.26% from 0.06 indicates that the surface changes from uniform to non-uniform profile distribution. For the grease-lubricated bearing, the skewness decreases consistently to -0.36, indicating the asperities peak were removed and the sharpness is lesser. The R_{ku} value increases by 67.06% and 29.41% for un-lubricated and lubricated bearing respectively, showing the surface has many high peaks and low valleys. This finding indicates that skewness and kurtosis parameters show a better representation of rough surfaces and can differentiate between surfaces having different shapes but similar R_a value.

(b) Comparison between dry un-lubricated and grease-lubricated condition shows that the un-lubricated bearing condition accelerated the bearing failure as severe surface damage was observed with noise and spark produced after operating for 1.5 hours. This includes a formation of material accumulation, surface roughening, and indentation as observed in surface topography. With grease lubrication, 0.79 μm of film thickness is formed between two contacting surfaces and eliminates the material particles produced during rolling contact. With lubrication, bearing failure has been delayed and prolong the bearing life up to 100 hours of operation.

ACKNOWLEDGMENT

The authors gratefully acknowledge the financial support of Universiti Sains Malaysia in providing the Short-Term Grant research fund (304/PMEKANIK/6315295) and workspace to complete this study

REFERENCES

Abbott, E.J., Firestone, F.A. (1933). Specifying surface quality - a method based on accurate measurement and comparisozugeln. *Mechanical Engineering, 55, 556-572.*

Archard, J. F. (1957). Elastic deformation and the laws of friction. *Proceedings of the Royal Society of London. Series A. Mathematical and Physical Sciences*, *243*(1233), 190-205.

Berthe, L., Sainsot, P., Lubrecht, A. A., & Baietto, M. C. (2014). Plastic deformation of rough rolling contact: An experimental and numerical investigation. *Wear*, *312*(1-2), 51-57.

Zugelj, B. B., & Kalin, M. (2020). Submicron-scale experimental analyses of the multi-asperity contact behaviour of various steels, an aluminium alloy and a polymer. *Tribology International*, *141*, 105955.

Bruce, R. W. (2010). CRC Handbook of Lubrication: Theory and Practice of Tribology, Volume II: Theory and Design: CRC Press.

Bryant, M. J., Evans, H. P., & Snidle, R. W. (2012). Plastic deformation in rough surface line contacts—a finite element study. *Tribology International*, *46*(1), 269-278..

Bush, A. W., Gibson, R. D., & Thomas, T. R. (1975). The elastic contact of a rough surface. *Wear*, *35*(1), 87-111.

Cabanettes, F., & Rosén, B. G. (2014). Topography changes observation during running-in of rolling contacts. *Wear*, *315*(1-2), 78-86.

Clarke, A., Weeks, I. J. J., Snidle, R. W., & Evans, H. P. (2016). Running-in and micropitting behaviour of steel surfaces under mixed lubrication conditions. *Tribology International*, *101*, 59-68.

Gadelmawla, E. S., Koura, M. M., Maksoud, T. M. A., Elewa, I. M., & Soliman, H. H. (2002). Roughness parameters. *Journal of materials processing Technology*, *123*(1), 133-145.

Greenwood, J. A., & Williamson, J. P. (1966). Contact of nominally flat surfaces. *Proceedings of the royal society of London. Series A. Mathematical and physical sciences*, *295*(1442), 300-319.

Greenwood, J. A., Tripp, J. H. (1967). The elastic contact of rough spheres. ASME Journal of Applied Mechanics, 34, 153–159.

Groover, M. P. (2020). *Fundamentals of modern manufacturing: materials, processes, and systems*. John Wiley & Sons.

Hansen, J., Björling, M., & Larsson, R. (2019). Mapping of the lubrication regimes in rough surface EHL contacts. *Tribology International*, *131*, 637-651.

Ismail, R., Tauviqirrahman, M., & Schipper, D. J. (2011). Topographical change of engineering surface due to running-in of rolling contacts. In *New Tribological Ways*. IntechOpen.

Jamari, J., & Schipper, D. J. (2007). Deformation due to contact between a rough surface and a smooth ball. *Wear*, *262*(1-2), 138-145.

Jamari, J., & Schipper, D. J. (2007). Plastic deformation and contact area of an elastic–plastic contact of ellipsoid bodies after unloading. *Tribology International*, *40*(8), 1311-1318.

Johnson, K. L. (1995). Contact mechanics and the wear of metals. Wear, 190, 162-170.

Kucharski, S., & Starzyński, G. (2019). Contact of rough surfaces under normal and tangential loading. *Wear*, *440*, 203075.

Lee, W., Tokoroyama, T., Murashima, M., Umehara, N. (2019). Investigating running-in behavior to understand wear behavior of ta-C coating with filtered cathodic vacuum arc deposition. Jurnal Tribologi, 23, 38-47.

Mohd Yusof, N.F., Ripin, Z. M. (2014). Analysis of Surface Parameters and Vibration of Roller Bearing. Tribology Transactions, 57, 715-729.

Mohd Yusof, N.F., Ripin, Z. M. (2016), A technique to measure surface asperities plastic deformation and wear in rolling contact. Wear, 368–369, 496–504.

Olofsson, U. and Dizdar, S. (1998). Surface analysis of boundary-lubricated spherical roller thrust bearings. Wear, 215, 156–164.

Rasp, W. and Wichern, C. M. (2002). Effects of surface-topography directionality and lubrication condition on frictional behaviour during plastic deformation. Journal of Material Processing Technology, 125–126, 379–386.

Sahoo, P. (2011). Tribology for Engineers: Chapter 1: Surface topography, Woodhead Publishing.

Singh, K., Tiwari, M., Mahato, A. (2019). Fretting wear characteristics of AISI 1040 steel alloy. Jurnal Tribologi, 20, 65-73.

Sosa, M., Börklund, S., Sellgren, U., Olofsson, U. (2014). In situ surface characterization of running-in of involute gears. Wear, 340–341, 1–6.

Sosa, M., Sellgren, U., Björklund, S., Olofsson, U. (2016). In situ running-in analysis of ground gears. Wear, 352–353, 122–129.

Suh, A.Y., Polycarpou, A. A., Conry, T.F. (2003). Detailed surface roughness characterization of engineering surfaces undergoing tribological testing leading to scuffing. Wear, 255, 556–568.
Tomota, T., Kondoh, Y., Ohmori, T. (2019). Modeling solid contact between smooth and rough surfaces with non-gaussian distributions, Tribology Transactions, 62(4), 580-591.
Tomota, T. Masuda, R., Kondoh, Y., Ohmori, T., Yagi, K., (2020). Modeling solid contact between rough surfaces with various roughness parameters. Tribology Transactions.
Thomas, T. R. (1981). Characterization of surface roughness Precision Engineering, 3(2), 97–104.
Wang, Q. J., Chung, Y.W. (2013). Encyclopedia of Tribology, Springer.
Wei, X., Xuesong, L., Jianguo, Y., Hongyuan, F., Wenli, X. (2009). Effect of temperature on plastic deformation of sheet by electromagnetic force. Journal of Materials Processing Technology, 209(5), 2693-2698.
Welzel, F. (2009). Formation of mechanical sparks in sliding metal contacts. Proceedings of the 22nd International Colloquium on the Dynamics of Explosion and Reactive Systems.
Yastrebov, V. A., Durand, J., Proudhon, H., Cailletaud, G. (2011). Rough surface contact analysis by means of the finite element method and of a new reduced model, Comptes Rendus Mécanique, 339, 473–490.